

Metallic conductivity and metal-semiconductor transition in Ga-doped ZnO

V. Bhosle,^{a1} A. Tiwari, and J. Narayan

Department of Materials Science and Engineering, North Carolina State University, Raleigh, North Carolina 27695-7907

(Received 2 September 2005; accepted 18 December 2005; published online 18 January 2006)

This letter reports the metallic conductivity in Ga:ZnO system at room temperature and a metal-semiconductor transition (MST) behavior at low temperatures. Zn_{0.95}Ga_{0.05}O films, deposited by pulsed laser deposition in the pressure range of $\sim 10^{-2}$ Torr of oxygen, were found to be crystalline and exhibited degeneracy at room temperature with the electrical resistivity close to $1.4 \times 10^{-4} \Omega \text{ cm}$ and transmittance $>80\%$ in the visible region. Temperature dependent resistivity measurements of these highly conducting and transparent films also showed, for the first time, a MST at ~ 170 K. Mechanisms responsible for these observations are discussed in the terms of dopant addition and its effect on ionization efficiency of oxygen vacancies. © 2006 American Institute of Physics. [DOI: 10.1063/1.2165281]

The ever-increasing demand for transparent conducting oxides (TCO) for usage in flat panel displays, light emitting diodes (LEDs), photovoltaics, and architectural window applications, has been the primary motivation for research on TCOs.^{1,2} Currently, indium tin oxide (ITO) is used for most of the TCO applications because of its high transmittance in the visible region and resistivity close to $1.0 \times 10^{-4} \Omega \text{ cm}$.^{2,3} However, ITO usage has caused concerns because of the high cost of indium and its limited supply.³ In addition, diffusion barrier characteristics and thermal stability of ITO pose a problem for transparent electrodes in LEDs. ZnO doped with group-III impurities (e.g., Al and Ga) has shown promising results as a relatively inexpensive alternative TCO material with optical and electrical properties comparable to those of ITO.²⁻⁵ Some other materials which exhibit similar properties are Cd₂SnO₄, F:SnO₂, and Nb:TiO₂.^{6,7} The recent discovery of a transparent metal-Nb:TiO₂, which is transparent in the visible region and also shows a positive temperature coefficient of resistivity (TCR), has generated a lot of excitement and a stimulus to understand the carrier generation and transport in highly conductive TCOs.⁷ A transition from an insulating to a metallic system can be explained by the increase in carrier concentration and formation of a degenerate band due to doping, as suggested by Mott.⁸ However, in the case of highly conducting TCOs, where extrinsic as well as intrinsic donors are known to affect the carrier concentration and the conductivity, the exact nature and interdependence of these entities is far from understood. In this letter, we report the properties of highly degenerate Ga:ZnO thin films and their dependence on vacancies, whose ionization efficiencies were found to be dependent on extrinsic doping. In order to understand the fundamentals of carrier generation and transport characteristics, we have investigated the temperature dependence of the resistivity of Ga-doped ZnO thin films with varying vacancy concentrations. We present optical, structural, chemical, and electrical property measurements to understand interesting characteristics of Ga:ZnO films. The possible mechanisms responsible for the observation of metallic conductivity at room temperature and metal-semiconductor transition (MST) at lower temperatures in Zn_{0.95}Ga_{0.05}O film are discussed in terms of donor characteristics and ionization efficiency of oxygen vacancies,

which are found to be dependent on dopant concentration.

Zn_{0.95}Ga_{0.05}O films were grown on *c*-plane sapphire single crystal substrates by pulsed-laser deposition (PLD).⁹ The gallium-doped ZnO target used was prepared by the conventional solid-state reaction technique. A pulsed KrF excimer laser with a wavelength of 248 nm was used for ablation. The energy density of the laser beam was varied from 4–7 J/cm² with a repetition rate of 10 Hz. The chamber was evacuated to a base pressure of 1×10^{-3} Torr, and the deposition was carried out at 2×10^{-2} Torr of oxygen pressure. The deposition was performed in the temperature range of 400–450 °C for 12 min. For comparison of the properties, pure ZnO films were also grown under similar deposition conditions. To investigate the effect of oxygen concentration on the film properties, films were deposited under higher oxygen pressure (1×10^{-1} Torr). In addition, films were also annealed in air at 600 °C for 15 min to study the same. X-ray diffraction (XRD) (θ - 2θ scan) of the films was carried out using a Rigaku X-ray diffractometer with Cu *K* α radiation ($\lambda = 1.54 \text{ \AA}$) and a Ni filter. A JEOL-2010 field emission transmission electron microscope (TEM) with an attached gatan image filter was used to perform the structural characterization of the film. X-ray photoelectron spectroscopy (XPS) was performed using a Riber LAS-3000 instrument with a Mg *K* α x-ray source. Analysis of the oxidation states from the spectrum was performed by deconvolution using Shirley routine and Casa software.¹⁰ The values corresponding to the C 1s peak were used as reference for the curve fitting analysis. Optical measurements (absorption/transmission) were made using a Hitachi U-3010 Spectrophotometer, while the electrical resistivity was measured using the four-point probe technique.

Figure 1 shows an XRD trace for the film grown at 400 °C and 2.4×10^{-2} Torr of oxygen pressure, which shows that the films are highly textured along the *c* axis and aligned with the (0006) peak of sapphire. The absence of additional peaks in the XRD pattern excludes the possibility of any extra phases and/or large-size precipitates in the films. Further structural details were obtained using high-resolution TEM (HRTEM) and selective area electron diffraction (SAED) patterns. Film thickness was determined to be ~ 240 nm, from a low magnification cross-sectional TEM image shown in Fig. 2(a). From Fig. 2(b), which is a HR-TEM image, it can be seen that the ZnO film has grown

^{a1}Electronic mail: vmbhosle@ncsu.edu

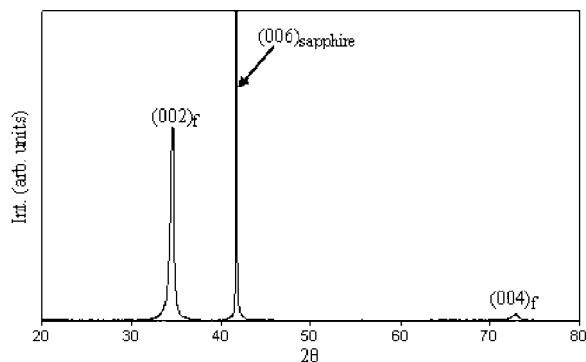


FIG. 1. XRD of the $\text{Zn}_{0.95}\text{Ga}_{0.05}\text{O}$ film deposited at 400°C and 2×10^{-2} Torr of oxygen.

epitaxially on sapphire and is free of any nanosized clusters or precipitates, which might have been difficult to detect by XRD. SAED taken from the interface is shown as an inset in Fig. 2(b), and illustrates the following epitaxial relationship: $(0002)_f \parallel (0002)_s$, $(\bar{2}110)_f \parallel (01\bar{1}0)_s$, $(01\bar{1}0)_f \parallel (\bar{2}110)_s$. This epitaxial relationship corresponds to a 30° or 90° rotation in the basal plane of the sapphire (0001) substrate. The epitaxy in such a large (16%) misfit system occurs as a result of domain matching epitaxy, where integral multiples of film planes, $6(01\bar{1}0)_f$ match with $7(\bar{2}110)_s$ of the substrate planes.¹¹ Chemical analysis of the film was performed using XPS to determine the extent and nature of gallium solubility in ZnO. From a high-resolution XPS spectrum, the positions of

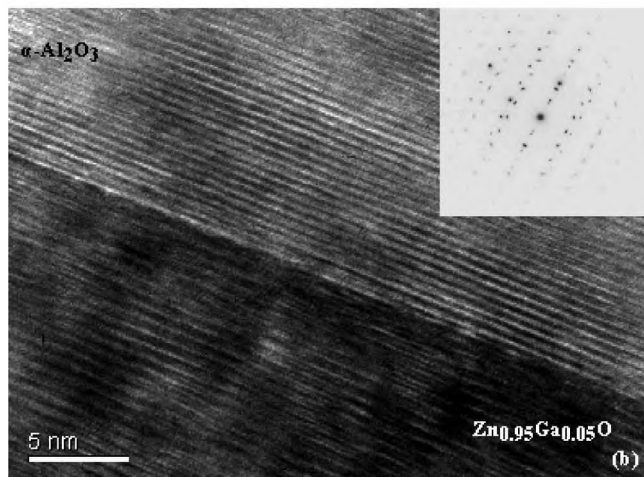
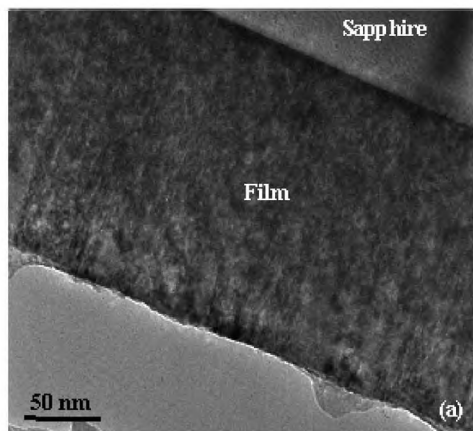


FIG. 2. (a) Low magnification image of the film on sapphire. (b) HRTEM of the interface and the inset showing the SAED of the same.

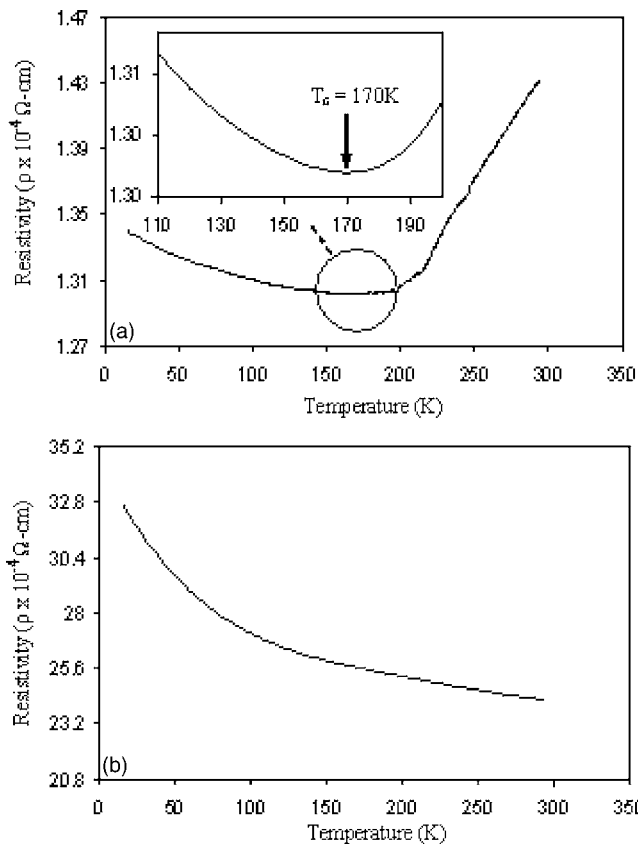


FIG. 3. Plot of resistivity vs temperature for (a) $\text{Zn}_{0.95}\text{Ga}_{0.05}\text{O}$ film grown at 2×10^{-2} Torr of oxygen and (b) 1×10^{-1} Torr of oxygen.

Ga $2p_{3/2}$ and Ga $2p_{1/2}$ peaks were found to be at 1119.0 eV and 1146.2 eV, respectively. These peak positions are in good agreement with the previously reported values,¹² which suggest that gallium exists as Ga^{3+} . The absence of gallium oxide clusters, as observed from the HRTEM and XRD analyses, indicates that Ga^{3+} occupies Zn substitutional sites and, therefore, can act as an effective donor.

The effect of doping was studied by measuring the electrical and optical properties of the films grown under different conditions. Figure 3 shows the effect of oxygen pressure on the temperature dependence of resistivity for Ga-doped ZnO films. Figure 3(a) corresponds to the film grown at 2×10^{-2} Torr of oxygen pressure, which shows a MST: Metallic conductivity above ~ 170 K, and semiconducting behavior at temperatures below it, as can be clearly seen in the inset. Room-temperature resistivity of this film was determined to be $1.4 \times 10^{-4} \Omega \text{ cm}$. Pure ZnO grown under similar conditions and the doped films deposited in higher oxygen pressure, however, showed higher room-temperature resistivities and exhibited only semiconducting behavior. Figure 3(b) is the plot of resistivity versus temperature for the film grown in higher oxygen pressure (1×10^{-1} Torr) which has the resistivity of $2 \times 10^{-3} \Omega \text{ cm}$ at ambient temperatures. The resistivities of the films annealed at 600°C for 15 min and undoped ZnO were found to be on the order of $\sim 10^{-1} \Omega \text{ cm}$. These films also showed negative TCR: characteristic of semiconducting behavior. The metallic conductivity observed here can be explained by the formation of a degenerate band appearing in heavily doped semiconductors as suggested by Mott.⁸ Similar observations of high conductivities and positive TCR have also been reported in the case of Al:ZnO,^{13,14} Nb:TiO₂,⁷ and P: Si.¹⁵ The increase in conduc-

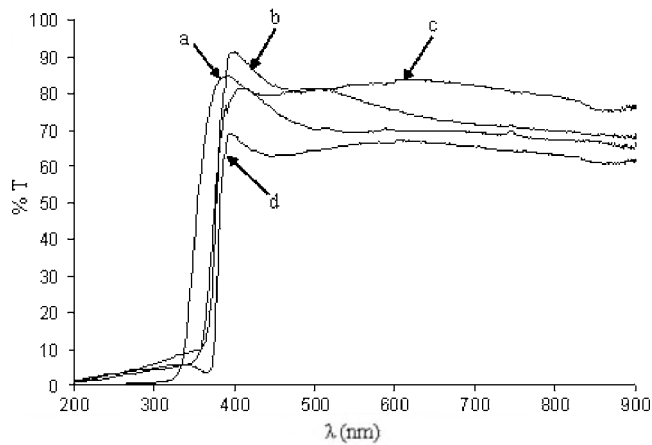


FIG. 4. Transmission spectra of (a) as-deposited $\text{Zn}_{0.95}\text{Ga}_{0.05}\text{O}$ film grown at 2×10^{-2} Torr of oxygen, (b) same film annealed in air at 600°C for 15 min, (c) as-deposited $\text{Zn}_{0.95}\text{Ga}_{0.05}\text{O}$ film grown at 1×10^{-1} Torr of oxygen, and (d) as-deposited ZnO film grown at 2×10^{-2} Torr.

tivity of ZnO thin films is a combined effect of Ga doping and oxygen vacancies, which act as donors and lead to degeneracy.^{16,17} However, the increase in resistivity—observed for annealed samples and for those grown in higher oxygen pressure—suggests that the oxygen vacancies are the major contributors to the increase in carrier concentration. The decrease in carrier concentration also shifts the Fermi level below the conduction band and thus explains the observed semiconducting behavior for these samples. The variation of carrier concentration is also manifested in Fig. 4, which illustrates the transmission spectra of the films deposited and processed under different conditions. The transmittance of all the films in visible region was found to be $\sim 80\%$. It can also be seen from the figure that for the film with the lowest resistivity, the absorption edge is shifted toward higher energy due to the Burstein–Moss effect.^{18,19} However, on annealing, the absorption edge moves to higher wavelength, indicating the decrease in carrier concentration due to reduction in the number of oxygen vacancies.^{17,20} Photoluminescence measurements also showed similar peak shifts, further strengthening our argument that the carrier concentration is increased partly due to the increased number of vacancies. It was observed that the PL peak corresponding to the film annealed in air showed a redshift due to the filling of vacancies and reduced carrier concentration, which is in agreement with the observed increase in resistivity and semiconducting nature of this film.

Although, vacancies play an important role in lowering the resistivities in Ga-doped ZnO, they are not as effective in pure ZnO, since pure ZnO grown under a similar growth condition showed considerably higher resistivity and also exhibited semiconducting behavior. This indicates that the energy levels of oxygen vacancies in ZnO are effected to a certain extent by dopants, such as gallium. Thus, gallium not only acts as an effective donor, but also changes the oxygen vacancy characteristics, which leads to very low resistivities. In addition, gallium also tends to affect the carrier transport, as is evident at low temperatures. The presence of impurity atoms, such as gallium, can lead to disorder in a degenerate semiconductor, resulting in localization of the electronic states²¹ and corresponding increase in resistivity with a negative TCR, as observed in Fig. 4(a). However, at temperatures higher than the transition, electrons are delocalized due to

thermal activation, and the conductivity is dominated by phonon scattering. Further work is needed in order to fully understand the effect of gallium on electrical properties of ZnO, especially at low temperatures.

In conclusion, we have grown highly conducting and transparent gallium-doped ZnO thin films on sapphire by PLD. For 5 at. % Ga-doped samples, the resistivity value is close to $1.5 \times 10^{-4} \Omega \text{ cm}$ and the transmittance is $\sim 80\%$. Such low resistivities and high transmittances were achieved with an optimized combination of dopant and oxygen vacancy concentration. In addition, this is the first time that metallic conductivity with a metal-semiconductor transition has been observed in gallium-doped ZnO. Detailed structural characterization confirms the epitaxial nature of the films and also suggests the absence of extra phases and/or nanoclusters. XPS analysis reveals that gallium is present as Ga^{3+} and, therefore, can act as an effective donor. The high conductivity observed arises from the interactions of oxygen vacancies and the gallium dopants. Oxygen vacancies increase the carrier concentration considerably, but, the energy levels or the ionization efficiencies of these vacancies depend on the dopant, such as gallium, present in the ZnO matrix. The room-temperature properties of Ga-doped ZnO rival those of commercially available ITO, which makes it a promising candidate for various TCO applications. Also, the metallic nature and the MST observed at low temperatures in ZnO due to gallium doping are certainly intriguing and further work is needed to understand these phenomena completely, which could give insight into the transport characteristics of TCOs with low resistivities.

This work was supported by NSF and NRO.

- ¹D. S. Ginley and C. Bright, *MRS Bull.* **25**, 15 (2000).
- ²T. Minami, *MRS Bull.* **25**, 38 (2000).
- ³T. Minami, *Semicond. Sci. Technol.* **20**, S35 (2005).
- ⁴A. Suzuki, T. Matsushita, T. Aoki, Y. Yoneyama, and M. Okuda, *Jpn. J. Appl. Phys., Part 2* **38**, L71 (1999).
- ⁵H. Hirasawa, M. Yoshida, S. Nakamura, Y. Suzuki, S. Okada, and K. Kondo, *Sol. Energy Mater. Sol. Cells* **67**, 231 (2001).
- ⁶R. G. Gordon, *MRS Bull.* **52**, 15 (2000).
- ⁷Y. Furubayashi, T. Hitosugi, Y. Yamamoto, K. Inaba, G. Kinodo, Y. Hirose, T. Shimada, and T. Hasegawa, *Appl. Phys. Lett.* **86**, 252101 (2005).
- ⁸N. F. Mott, *Metal-Insulator Transition* (Taylor and Francis, London, 1974).
- ⁹D. B. Chrisey and G. H. Hubler, *Pulsed Laser Deposition of Thin Films* (Wiley, New York, 1994).
- ¹⁰<http://www.casaxps.com>; N. Fairley and A. Carrick, *The Casa Cookbook. Part 1 Recipes for XPS Data Processing* (Acolyte Science, Cheshire, UK, 2005).
- ¹¹J. Narayan and B. C. Larson, *J. Appl. Phys.* **93**, 278 (2003).
- ¹²M. Passlack, E. F. Schubert, W. S. Hobson, M. Hong, N. Moriya, S. N. G. Chu, K. Konstadinidis, J. P. Mannaerts, M. L. Schnoes, and G. J. Zydzik, *J. Appl. Phys.* **77**, 686 (1995).
- ¹³R. C. Budhani, P. Pant, R. K. Rakshit, K. Senapati, S. Mandal, N. K. Pandey, and J. Kumar, *J. Phys.: Condens. Matter* **17**, 75 (2005).
- ¹⁴J. Han, P. Q. Mantas, A. M. R. Senos, *J. Eur. Ceram. Soc.* **21**, 1883 (2001).
- ¹⁵M. Alexander and D. F. Holcomb, *Rev. Mod. Phys.* **40**, 815 (1968).
- ¹⁶B. H. Choi, H. B. Im, J. S. Song, and K. H. Yoon, *Thin Solid Films* **193**, 712 (1990).
- ¹⁷D. H. Zhang and D. E. Brodie, *Thin Solid Films* **213**, 109 (1992).
- ¹⁸E. Burstein, *Phys. Rev.* **93**, 632 (1954).
- ¹⁹T. S. Moss, *Proc. Phys. Soc. London, Sect. B* **67**, 775 (1954).
- ²⁰S.-S. Lin, J. L. Huang, and P. Sajgalik, *Surf. Coat. Technol.* **185**, 254 (2004).
- ²¹N. F. Mott, *Conduction in Non-Crystalline Materials* (Clarendon, Oxford, 1993).